

Hydrophobically modified poly(vinyl alcohol) and bentonite nanocomposites thereof: Barrier, mechanical, and aesthetic properties

Caisa Johansson,¹ Francis Clegg²

¹Department of Engineering and Chemical Sciences, Faculty of Health, Science and Technology, Karlstad University, SE-651 88 Karlstad, Sweden

²Materials and Engineering Research Institute, Sheffield Hallam University, Sheffield, S1 1WB, United Kingdom

Correspondence to: C. Johansson (E-mail: caisa.johansson@kau.se)

ABSTRACT: Composite films were formed by incorporating three different bentonites into an ethylene modified, water-soluble poly(vinyl alcohol), EPVOH. The interaction of EPVOH with both hydrophilic and hydrophobic bentonites was investigated. EPVOH provided lower water vapor and oxygen transmission rates compared to a conventional PVOH grade when exposed at high relative humidities (70–90% RH). EPVOH films which exhibited oxygen barrier properties comparable to that of a biaxially oriented PET packaging film at 80% RH were produced. High compatibility between EPVOH and hydrophilic bentonites provided an even distribution of clay platelets in the composites. A strong increase in Young's modulus with increased addition of any of the three bentonites was found. At low addition levels the hydrophobic bentonite proved to be effective in terms of maintaining high elongation at break, high transparency and high gloss. © 2014 Wiley Periodicals, Inc. *J. Appl. Polym. Sci.* **2015**, *132*, 41737.

KEYWORDS: clay; composites; films; mechanical properties; packaging

Received 4 September 2014; accepted 8 November 2014

DOI: 10.1002/app.41737

INTRODUCTION

Poly(vinyl alcohol), PVOH, is a synthetic polymer that offers good film-forming and coating properties and the films or coatings produced are proven effective barrier materials to oxygen and other gases. PVOH has also been widely used as a model polymer for studying properties of hydrophilic polymers, due to its simple and well-defined chemical structure.^{1,2}

The hydrophilic PVOH is sensitive to moisture and thus its barrier properties are strongly affected by the surrounding relative humidity (RH). For instance the oxygen permeability of PVOH films generally increases 2500 times on going from 0 to 100% RH.³ This is typical of hydrophilic (bio)polymers in which their oxygen permeability increases exponentially with increased relative humidity.⁴ The loss of oxygen barrier under moist conditions is therefore one of the major obstacles preventing the successful use of these polymers in the food packaging sector, especially for packaging high-moisture foods or food which will rapidly lose quality when in contact with moisture or oxygen. Knowledge generated from studies on PVOH may ultimately lead to novel approaches to improve its performance and that of other hydrophilic biobased polymers, e.g. starch, for use in packaging applications.⁵

PVOH allows a wide range of chemical modifications to its backbone. Consequently, critical parameters such as molecular weight and solution viscosity can be tuned to match the specifications

required for different applications. Several attempts have been made to improve the barrier properties of PVOH when exposed at high relative humidities by, for example, copolymerization of vinyl alcohol and ethylene. The resulting ethylene vinyl alcohol (EVOH) copolymers are known for their outstanding gas barrier properties, which are much superior to other polymers conventionally used in packaging. The highest oxygen barrier properties of EVOH occur with ethylene in the range of 27–32 mol %.⁶ However, the poor water solubility of EVOH copolymers at these high ethylene contents restricts their utility to water-free processes like extrusion coating and blow molding.^{6,7} Consequently, water-soluble ethylene modified random copolymers of poly(vinyl alcohol) have recently been introduced to the market under the trade name Exceval[®] (herein termed EPVOH). The ethylene modification gives the polymer a hydrophobic character. EPVOH is stated to have lower oxygen transmission rates (OTR) than standard PVOH films by almost an order of magnitude,⁸ moreover they are also more effective oxygen barriers at higher relative humidities. These water-soluble EPVOHs are also claimed to have OTR values below that of commercial, non-water soluble EVOH coatings (27 mol % ethylene) in the range from zero to 70% RH.⁸ Thus, their water-solubility, biodegradability, favorable barrier properties and approval for food contact make these novel grades highly exploitable for use as films or coatings for various food packaging applications.

Another strategy to improve the barrier and mechanical performance of polymer films is the formation of composites by the incorporation of mineral fillers, especially layered silicate minerals like montmorillonite. Compatibility between polymer and mineral filler is crucial for the formation of well-dispersed composite structures.^{9,10} Intercalation or exfoliation of clay layers are favored if the hydrophilicity/hydrophobicity of the polymer and the natural (unmodified) or organically modified clay are closely matched.¹¹ Organophilic modification of clays by replacing the naturally occurring exchangeable alkali or alkaline earth metal ions with organic cations lowers the surface energy of the clay and increases their compatibility with a number of hydrophobic polymer matrices.^{12–14}

Successful intercalation or exfoliation of hydrophilic hectorite and montmorillonite in water-soluble PVOH has been reported e.g. by Carrado *et al.*¹⁵ and Strawhecker and Manias,¹⁶ whereas addition of hydrophobic organomodified clays to hydrophilic starch led to the formation of microcomposites.^{11,17,18} Natural montmorillonites are easily dispersed in water due to their polar character¹⁰ and are thus in general compatible with water-soluble polymers like PVOH. A convenient and widely accepted method for composite formation and preparation of coatings is therefore by solvent mixing/casting even though melt intercalation may be considered the most conventional.¹²

Transparency is frequently demanded for polymer films used in packaging^{19,20} as brand owners want customers to be attracted by the visual aspect of their product. The addition of fillers visually makes composite films more opaque and the quality and level of filler addition that still provides acceptable transparency are thus important issues when selecting filler materials. Layered silicate minerals have gained interest as fillers for PVOH films as a way to retain their optical clarity, which is contrary to conventional fillers that generate opaque films.¹⁶ However, most clays have a natural off-white to yellowish color and their effect on the overall visual perception of colorless polymer films needs to be assessed.

In this study, a conventional PVOH and two EPVOH grades were investigated. Three different bentonites, as fillers, were incorporated at selected concentrations to form composite films. Because application of water dispersions is a widely adopted method for coating of paper for packaging manufacture, this study concentrated on the formation of composite films using water as solvent. One of the major objectives was to study how the water-soluble hydrophobically modified EPVOHs interacted with both hydrophilic (natural) and organophilic (organomodified) clays. The molecular weight and chemical composition of the polymers were first characterized. Then the hydrophobic character of cast films was analyzed in terms of polar/apolar surface energy. The water vapor and oxygen transmission rates were determined after exposure to various relative humidities (RH). In addition, the influence of filler type and concentration on mechanical properties, transparency, color and gloss of composite films were evaluated.

EXPERIMENTAL

Materials

Poly(vinyl alcohol) with degree of hydrolysis, DH, of 98–99 mol % was used as the standard, unmodified PVOH grade. An

EPVOH development product (here denoted EPVOH) was used to study the impact of the hydrophobic modification on the barrier properties. A commercial EPVOH grade (here denoted EPVOHc) was used for reference. Both EPVOH and EPVOHc had DH values in the range 97.5–99 mol %. All three grades were supplied by Kuraray Europe GmbH (Frankfurt am Main, Germany).

Polyethylene (LDPE 30 μm , defa-Folien/Heikoflex, Lohmar, Germany) and polyethylene terephthalate (PET 12 μm , biaxially oriented Hostaphan[®], Mitsubishi Polyester film, Wiesbaden, Germany) films were used for reference. These polymers are universal food packaging films with well-defined structures. The oxygen permeability of the LDPE and PET films are considered to be unaffected by relative humidity due to their nonpolar character.²¹

Three different bentonites each containing predominantly montmorillonite were used: (i) Cloisite[®]Na⁺, (here denoted Na-MMT) from Southern Clay Products, Gonzales, TX with a cation exchange capacity (CEC) of 92.6 meq/100 g clay and layer diameter of 75–100 nm, (ii) PGN[®] from Nanocor, Arlington Heights, IL, which mostly contains Na⁺ exchangeable cations but also a small portion of Ca²⁺ (here denoted C-MMT). More significantly, C-MMT has a larger layer diameter of 300–500 nm and a higher CEC value (120 meq/100 g) compared to Na-MMT, (iii) Dellite[®] 67G (Laviosa Chimica Mineraria S.p.A., Livorno, Italy), which is an organically modified bentonite (here denoted Q-MMT) in which the naturally occurring sodium ions have been replaced by dimethyl-dihydrogenated tallow ammonium ions. Q-MMT has a cation exchange capacity of 105 meq/100 g clay and a layer diameter of 500 nm. Both Na-MMT and C-MMT are intended for use as additives to hydrophilic polymers such as polyvinyl alcohols, polysaccharides and polyacrylic acids, whereas Q-MMT is intended for hydrophobic polymers including polypropylene, polyethylene or ethylene vinyl acetate.

Methods

All three polymers were dissolved in water at 10 wt % and heated at 95°C for 60 min whilst being continuously stirred. Bentonites were used without pre-treatment and polymer-clay composites were formed by addition of 3, 6, 9, or 12 parts dry clay per hundred parts of dry polymer whilst heating. Additional water was added to adjust the final solids content to 10 wt % in all mixtures.

Characterization of Polymers

The molecular weight of the polymers was determined using a size exclusion chromatography (SEC) device fitted with a Waters 410 Refractive Index Detector. Samples were dissolved in the mobile phase (10 mM NaOH in Milli-Q water) at 10 mg mL⁻¹ and filtered through a 0.45 μm PTFE syringe filter prior to analysis. The samples were injected using a 20 μL sample loop (Rheodyne 7725 Manual Injector) and a Waters 515 HPLC pump operated at a flow rate of 1 mL min⁻¹. The columns used were Tosoh TSKGel (G3000PW-G4000 PW-G3000PW) with guard column TSKGel (PWL 7.5 cm \times 7.5 mm). Calibration was achieved using polyethylene glycol/polyethylene oxide

standards with molecular weights ranging from 1500 to 250,000 g mol⁻¹.

The solution viscosities of the 10 wt % polymer solutions were determined by a Brookfield viscometer (Brookfield Viscometers, Essex, UK) operated at 100 rpm (spindle no. 4) for comparison with molecular weight data.

Proton NMR (Bruker AC 250 spectrometer, Bruker Corporation) was used to determine the ethylene content in the EPVOH and EPVOHc. The polymer samples were dissolved in D₂O to a concentration of 5 wt % at 95°C.

The viscosity of polymer-clay dispersions were recorded at 23°C using a controlled shear stress rheometer (Physica MCR 300, Physica Messtechnik GmbH, Ostfildern, Germany) in concentric cylinder geometry at shear rates in the range 1–4000 s⁻¹.

Film Casting and Measurement of Thickness

Films were cast by pouring 10.0 g polymer solution or EPVOH-clay dispersion in polystyrene Petri dishes with a diameter of 90 mm, followed by drying at 23°C and 50% RH for at least 5 days before any of the further treatments described below. Different film thicknesses were prepared by casting films using 10 wt % solutions further diluted with deionized water to produce 2, 4, 6, and 8 wt % solutions. Average film thicknesses were recorded using a thickness tester (Lorentzen & Wettre type 532 G, Stockholm, Sweden) at a minimum of five locations on each film. After studying the effect of film thickness a size of 100 μm was chosen for analysis of selected film properties since water vapor- and oxygen transmission rates were found to reach a plateau level, i.e. further increases in film thickness led to no significant improvement. Reproducible and identical film thicknesses were achieved independently of polymer-clay composition.

Water Vapor Transmission Rate

Water vapor transmission rates (WVTR) were measured by the gravimetric cup method (ASTM E96) using silica gel as desiccant and a climate chamber (C+10/200, CTS Clima Temperatur Systeme GmbH, Hechingen, Germany). Aluminum cups fitted with sample holders (lids) giving an exposed film area of 50 cm² were used. The cups were firmly tightened by placing a rubber O-ring on one side of the film whereas silicon grease was used to prevent leakage between the film and the aluminum ring on the other side. Initial measurements with films of different thickness were carried out at 23°C and 50 or 80% RH. Measurements were then performed on films with thickness of 100 μm at 23°C and with step-wise increases in relative humidity from 50 to 90% RH at 10% increments; the films were pre-conditioned for 16 h at each RH level.

Oxygen Transmission Rate

Oxygen transmission rates (OTR) were measured according to ASTM D3985-05 using a Mocon® OxTran® oxygen transmission rate tester, Model 2/21 (Mocon, Minneapolis, MA), equipped with a coulometric oxygen sensor. An adhesive aluminum foil mask was used to envelop the films, leaving an exposed test area of 5 cm². The oxygen concentration in the test gas was 21% and the carrier gas was a blend of 98% nitrogen and 2% hydrogen. Measurements were carried out in duplicates at a constant temperature of 23°C and atmospheric pressure.

The pure polymeric films were tested under step-wise increases in RH from 50 to 90% at 10% increments by adjustment of the test gas and carrier gas humidifiers so that the same RH level was achieved on both sides. The accuracy of the RH sensor was ±3%. Samples were pre-conditioned in the test chambers for 10 h at each RH level and measurements were performed until steady state was reached. The EPVOH-clay composite films were then tested at 50 and 80% RH.

Hydrophobic Character of Film Surfaces

The hydrophobic character of dry polymer films was assessed by recording the static contact angle (θ) of small liquid drops applied on the film surface at 23°C and 50% RH using a FTA 200 Dynamic Contact Angle Analyzer (First Ten Angstroms, Portsmouth, NH). The spreading of the drop over the film surface was captured using a CCD camera over a time period from 0 to 80 s. All pure polymeric films were analyzed using three test liquids with varying polarity: deionized water and ethylene glycol (anhydrous, VWR International), were applied with a drop volume of 10 μL, whereas methylene iodide (Fluka Chemika GmbH, Switzerland) used a drop volume of 2.0 μL. Average contact angles were calculated from six replicates at the point where the contact angle versus time curves leveled out after the initial spreading period. This point was reached after about 10 s in the case of ethylene glycol and water whereas the contact angle was virtually constant over the whole test period in the case of methylene iodide. The resulting film surface energies γ_s were calculated from the Young-Dupré equation, eq. (1), by inserting the different Lifshitz-van der Waals γ_i^{LW} dispersive interaction components (apolar character), and the electron acceptor, γ_i^+ (acidic) and electron donor γ_i^- (basic) surface energy components of the test liquids.²² The latter two components together form the Lewis acid-base interactions $\gamma^{AB}=2\sqrt{\gamma^+\gamma^-}$ (polar character). The subscripts *s* and *l* represents solid and liquid, respectively.

$$\gamma_l(1 + \cos\theta) = 2 \left(\sqrt{\gamma_s^{LW}\gamma_l^{LW}} + \sqrt{\gamma_s^+\gamma_l^-} + \sqrt{\gamma_s^-\gamma_l^+} \right) \quad (1)$$

The surface energies of the EPVOH-clay composite films were determined using only those with highest filler content (12 pph), whilst contact angle measurements with deionized water were determined for all EPVOH-composite films and expressed as the normalized contact angle relative to the pure EPVOH film.

Mechanical Properties

Test pieces of width 5 mm and length 60 mm were cut from the films of 100 μm thickness. The tensile strength (stress at break, σ_b) in MPa, elongation (strain at break, ϵ_b) in % and the Young's (initial) modulus, *E* (MPa) were recorded on a Zwick/Roell tensile tester, model Z005 (Zwick GmbH, KG, Ulm, Germany) with a load cell of 500 N. The distance between the clamps was 20 mm and the test speed was 100 mm min⁻¹. Testing was carried out at 23°C and 50% RH (i.e., no change compared to film preparation) for 12 test pieces from each film type.

Film Transparency, Reflectance, and Gloss

The transparency and reflectance of the films was recorded using a Minolta CM-3630 spectrophotometer (Minolta, Japan). Spectral reflectance curves were recorded in triplicate over the

Table I. Selected Properties of Poly(vinyl alcohol) Grades

Polymer	M_W (g mol ⁻¹)	M_N (g mol ⁻¹)	P_D	Viscosity (m Pa ⁻¹ s ⁻¹)
PVOH	71,500	35,500	2.01	980
EPVOH	61,200	32,300	1.80	870
EPVOHc	60,700	33,100	1.78	840

range 360–740 nm using a D65/10° illuminant with the top film surface directed towards the light source exposing an illumination area (\emptyset) of 30 mm. The transparency was evaluated by measuring the reflectance factor (%) of the films over a neutral white background, R_w , and the reflectance factor (%) over a black background, R_0 . The transparency T is defined by eq. (2):

$$T = \sqrt{(R_w - R_0) \cdot \left(\frac{10\,000}{R_w} - R_0 \right)} \quad (2)$$

An opaque sheet of a matte, pigment coated paperboard was used as the neutral white background with reflectance factor R_w . The reflectance and color of composite films was measured over the white background and the reflectance values at each wavelength for the white background itself was subtracted before evaluation (i.e., $R_w - R_w$). The reflectance and color of the clay minerals was recorded by the same technique. A portion of each clay grade was close-packed into a Petri dish to form a planar, smooth layer on the bottom. The dishes were tightly closed and the optical properties were evaluated by inserting the dish in the spectrophotometer with the planar bottom facing the incident light. An empty Petri dish was used for blank measurements. The color was evaluated in terms of the CIELAB color space L^* , a^* , and b^* values, where L^* represents the lightness and a^* and b^* are the chromaticity coordinates on the red-green and the yellow-blue axis respectively.

The gloss of films was recorded using a Zehntner ZGM 1022 gloss meter (Zehntner GmbH Testing Instruments, Hoelstein, Switzerland), at an incident angle of 20° according to ISO 8254-3, applicable for highly glossy surfaces. The gloss was recorded at six points on the top surface of each film with a measurement area of 44.2 mm².

RESULTS AND DISCUSSION

Characterization of Polymers

PVOH exhibits ~15% higher weight average molecular weight (M_W) and ~11% higher polydispersity index (P_D) compared to the EPVOH grades (Table I). The recorded viscosity of 10 wt % solutions followed the variations in M_W . The number average molecular weights (M_N) were however very close between the three grades (only ~9% and ~7% higher for PVOH than for EPVOH and EPVOHc, respectively); hence any observed variations in properties in this study has been attributed to the different chemical compositions, rather than the small differences in molecular weight.

The molecular structure of PVOH contains both vinyl acetate and vinyl alcohol groups and the formula can thus be written $-\text{[CH}_2\text{-CH(OCOCH}_3\text{)]}_m\text{-[CH}_2\text{-CH(OH)]}_n\text{-}$. In addition,

EPVOH and EPVOHc contains ethylene groups and their formula can thus be written $-\text{[CH}_2\text{-CH(OCOCH}_3\text{)]}_m\text{-[CH}_2\text{-CH(OH)]}_n\text{-[CH}_2\text{-CH}_2\text{]}_o\text{-}$, where the suffixes m , n , and o corresponds to the number of each unit.⁸ Note that the degree of hydrolysis, i.e. the fraction of vinyl acetate at 1–2.5 mol % is similar for all grades. The relative amounts of ethylene were estimated by ¹H NMR, the chemical shifts of selected peaks and their intensities are presented in Table II.

A broad range of peaks at 1.4–1.7 ppm were assigned to the methylene ($-\text{CH}_2$) protons of the vinyl alcohol units, $-\text{CH}_2\text{-CH(OH)-}$, in both PVOH and EPVOH and the protons of ethylene units, $-\text{CH}_2\text{-CH}_2\text{-}$, in the EPVOH. This observation is in line with Bastow *et al.* who reported methylene peaks at 1.65 ppm for PVOH²³ and de Souza and Tavares who identified the corresponding peaks for PVAc at 1.64 and 1.71 ppm.²⁴ Broad peaks centered at 3.9 ppm were attributed to the methine group of vinyl alcohol, $-\text{CH}_2\text{-CH(OH)}$ in agreement with Bastow *et al.*²³ who reported it at 3.65 ppm and with tabulated data typically given at 3.3–4.0 δ .²⁵ The intensity of this peak was normalized for each sample. Three sets of very low intensity peaks were observed for all samples centered at 3.2, 3.4 and 3.6 ppm. These possibly originate from the methine groups associated with vinyl alcohol groups present as end groups or bonded with vinyl groups. The total intensity for these three small peaks was identical for PVOH and EPVOH but slightly lower for EPVOHc.

Combining the intensities of the sets of weak peaks between 3.2 and 3.6 ppm with the peak at 3.9 ppm and comparing with the peaks at 1.4–1.7 ppm show that the ratio of $-\text{CH}$ to $-\text{CH}_2$ in PVOH was close to 1:2, which is in line with the theoretically expected ratio.

The peak intensities between 1.4 and 1.7 ppm were about 10% higher than those at 3.9 ppm for both EPVOH grades when compared to the pure PVOH. Taking the calculated ratio of $-\text{CH}$ to $-\text{CH}_2$ of 1:2.02 from PVOH and subtracting the value 2.02 from the intensities of the 1.4–1.7 ppm peaks of EPVOH allowed the contribution from the ethylene groups to be calculated. By dividing the obtained values by the number of hydrogens in each unit, the mol % fraction of ethylene groups could be calculated. The resulting values were 8.1 mol % for EPVOH and 8.0 mol % for EPVOHc.

Dispersion Properties of EPVOH/Clay Blends

Fresh solutions were used for film casting and evaluation of dispersion properties even though the viscosity of the 10 wt % EPVOH solution was found to be stable at room temperature and did not change even after several months of storage. EPVOH blends containing Na-MMT and C-MMT also showed high viscostability and the dispersions remained visually homogeneous over several weeks at rest when stored in clear glass bottles at room temperature. However, the clay in Q-MMT/EPVOH blends was observed to settle almost immediately upon cessation of stirring and a significant fraction of the clay sedimented in the glass bottle after 24 h. The Q-MMT particles however were readily re-dispersed by reapplication of shear. This poor dispersibility of organomodified clays in hydrophilic

Table II. Chemical Shifts and Peak Intensities of the ^1H NMR Spectra

Chemical shift (ppm)	Peak intensity			Assignment
	PVOH	EPVOH	EPVOHc	
1.4–1.7	2.190	2.402	2.396	$-\text{CH}_2-\text{CH}(\text{OH})-$ in PVOH and EPVOH; $-\text{CH}_2-\text{CH}_2-$ in EPVOH
3.2	0.010	0.005	0.005	
3.4	0.023	0.027	0.012	$-\text{CH}_2-\text{CH}(\text{OH})$ associated with end groups in PVOH and EPVOH
3.6	0.023	0.023	0.022	
3.9	1.000	1.000	1.000	$-\text{CH}_2-\text{CH}(\text{OH})$ in PVOH and EPVOH

solvents or water-soluble polymer solutions is typical, as demonstrated, for example, by Chang *et al.*²⁶

The compatibility of each clay grade at 3 pph with EPVOH was assessed by monitoring their effect on the dispersion viscosity. Figure 1 shows that the addition of Na-MMT resulted in the highest viscosity at all shear rates in the range 10–4000 s^{-1} . This reflects strong PVOH-clay interactions and indicates a high structural network and entanglement between polymer and clay, it also suggests a high single clay layer separation, i.e. a higher degree of exfoliation. Addition of C-MMT resulted in slightly lower viscosity than that for Na-MMT and reflects the different properties of the clay, i.e. its CEC and layer dimensions. It should be noted that clay-platelet interactions (edge-platelet or edge-edge interactions) as well as clay-polymer interactions can contribute to increased viscosity. The effect of Q-MMT was almost negligible since the blend viscosity practically overlapped that of pure EPVOH at all shear rates. The observation suggests that the Q-MMT particles were dispersed as microparticles (stacked clay layers) and not exfoliated, in the aqueous polymer solution.

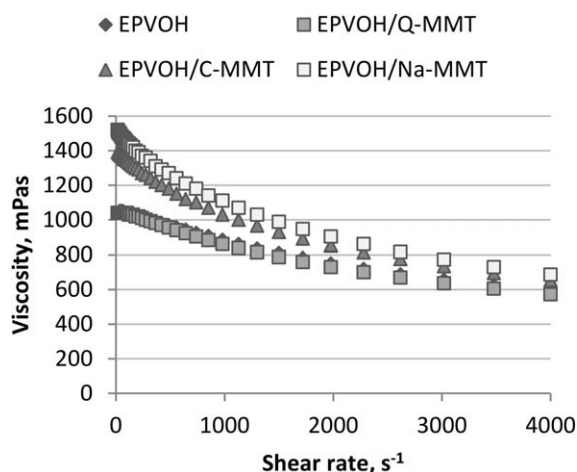
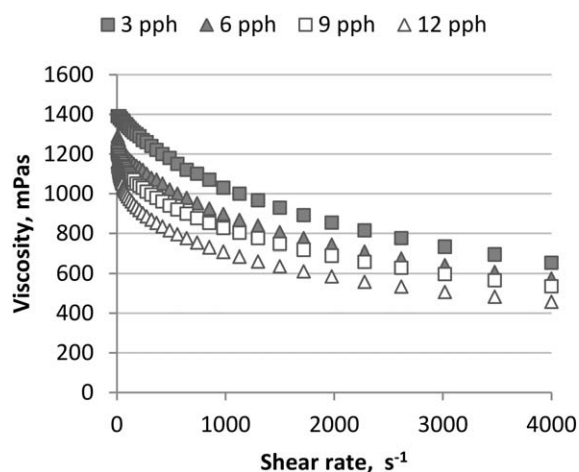
The pure EPVOH solution as well as all EPVOH-clay blends showed a shear thinning behavior over the range of shear rates investigated. Sinha Ray *et al.* showed that at high shear rates, the viscosity of poly(butylene succinate)-layered silicate nanocomposites were comparable to that of the pure polymer.²⁷

They suggested that the silicate layers are strongly oriented towards the flow direction at high shear rates, thus the flow properties are dominated by that of the pure polymer. The same explanation is believed to account for the behavior observed here.

The interrelationship among the three clays in terms of the viscosity effects depicted in Figure 1 was maintained also at addition levels of 6, 9, and 12 pph. However, for all three clays, a decrease in viscosity was found with increasing amounts of filler, which is illustrated by the data for the EPVOH/C-MMT blends in Figure 2.

Because the total solids content was kept constant in all formulations, the concentration of polymer decreased from 10.0 to 8.9 wt % as the clay concentration increased from 0 to 12 pph filler. It is known that the viscosity of aqueous solutions of fully hydrolyzed grades of poly(vinyl alcohol) increase rapidly with increased concentration.²⁸ For example, an increase from 2.5 to 15 wt % can result in a viscosity increase by a factor of 1000 for polymers with intermediate molecular weight. Entanglements between individual molecules are formed above a first critical concentration corresponding to 2–4 wt % and the formation of a completed network structure is assumed to occur above a second critical concentration, i.e., above 10–20 wt %.²⁸

A small change in polymer concentration may therefore have a large impact on the dispersion viscosity and so to assess this, a

**Figure 1.** Viscosity as a function of shear rate for EPVOH and EPVOH-clay blends comprising 3 pph filler.**Figure 2.** Viscosity as a function of shear rate for EPVOH/C-MMT blends.

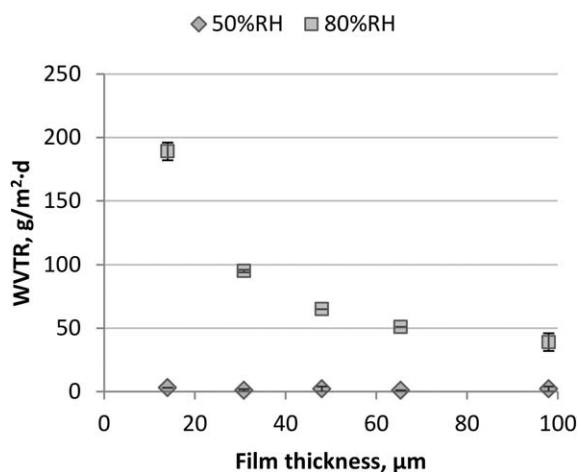


Figure 3. WVTR values of EPVOH films as a function of film thickness at two relative humidities and at 23°C. Average of three measurements. Error bars represents standard deviation.

separate experiment with continuous dilution of the EPVOH solution from 10 to 8 wt % was performed. A linear relationship between polymer concentration and viscosity was found at all shear rates investigated. Plotting the viscosity of the EPVOH/C-MMT blends against the actual concentration of polymer in the range 3–12 pph C-MMT revealed a linear relationship and the calculated relative viscosity ($\eta_{\text{blend}}/\eta_{\text{polymer}}$) was around 1.25 at 1000 s^{-1} and around 1.16 at 4000 s^{-1} for all clay addition levels, i.e. the viscosity profile mainly followed the polymer concentration and approached the viscosity of the pure polymer when the shear rate increased. For EPVOH/Na-MMT the relationship was linear only at the highest shear rates (above 1000 s^{-1}), which indicated a stronger interaction of Na-MMT with EPVOH at the lower shear rates. This means that higher shear forces are required to reach a point where a potential break-up of the network structure established between the Na-MMT particles and the polymer will take place. The corresponding $\eta_{\text{blend}}/\eta_{\text{polymer}}$ values for EPVOH/Na-MMT blends were 1.35 and 1.22 at 1000 and 4000 s^{-1} , respectively.

Obviously, the relative viscosities being >1 over the entire range of addition levels confirm that C-MMT and Na-MMT have an impact on the blend viscosity, i.e. the reduction in viscosity with increased amount of filler cannot solely be explained by a reduction in the polymer content. There is a decrease due to the decrease in polymer content, but this is offset (i.e., a relative increase in viscosity) by the addition of clay. The addition of clay is expected to increase viscosity, but the disruption of the polymer entanglement by the clay has a greater impact on the viscosity. Furthermore, the higher values of $\eta_{\text{blend}}/\eta_{\text{polymer}}$ for Na-MMT indicate stronger interactions with EPVOH for this clay grade over C-MMT.

Even though a decrease in viscosity was also found as the amounts of Q-MMT increased the EPVOH/Q-MMT blends displayed no linear relationship between the actual polymer concentration and viscosity at either low or high shear rates. The average $\eta_{\text{blend}}/\eta_{\text{polymer}}$ values were close to 1. This observation can be explained by a break-up or hindering of the formation

of entanglements of polymer chains by the presence of increased amount of clay dispersed in the polymer, thus leading to a decrease in apparent formulation viscosity, probably equally compensated by an increase in viscosity due to the addition of clay.

Investigation of the distribution of clay layers within dried composite films by means of XRD and FTIR confirmed that the observed variations in interaction between EPVOH and clays in the wet state had great impact on the final film properties.²⁹

It has been reported that layered silicates (not organomodified) remain in a colloidal suspension within an aqueous solution of PVOH; after slow drying (in air), they are embedded in a PVOH gel to form an exfoliated nanocomposite material.^{12,16} The same authors also state that after intense drying to remove all water (*in vacuo*) and with clay concentrations >5 –10 wt % the silicate layers re-aggregate to form intercalated structures (stacks) due to platelet-platelet attraction forces. Some single clay platelets however do not re-aggregate due to steric hindrance and remain disordered/exfoliated. At clay concentrations <5 –10 wt % intercalated structures are less apparent but the platelets are disordered and/or separated, which is due to the incorporation of higher quantities of PVOH between the layers overcoming the platelet-platelet attraction forces.

Water Vapor Transmission Rate

Figure 3 shows the effect of film thickness on WVTR values for the EPVOH films. It is evident that at 50% RH the transmission rate is almost independent of film thickness, whereas at 80% RH a steep decrease in WVTR values with increased film thickness is observed, which levels out at about 50 μm . The equilibrium moisture content in the films was 8.2 and 14.8% at these two relative humidities respectively.²⁹ The water vapor permeability (WVP) of the EPVOH films was calculated by dividing the recorded WVTR by the saturation vapor pressure at the actual test temperature and the RH gradient on each side of the

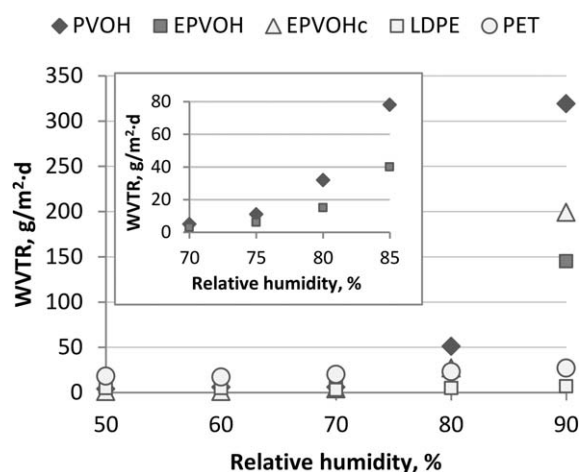


Figure 4. WVTR values as a function of relative humidity in the range 50–90% RH for PVOH, EPVOH grades (film thickness ~ 100 μm), together with that for the LDPE (30 μm) and PET (12 μm) reference films. WVTR values in the range 70–85% RH for PVOH and EPVOH (insert). Average of three measurements.

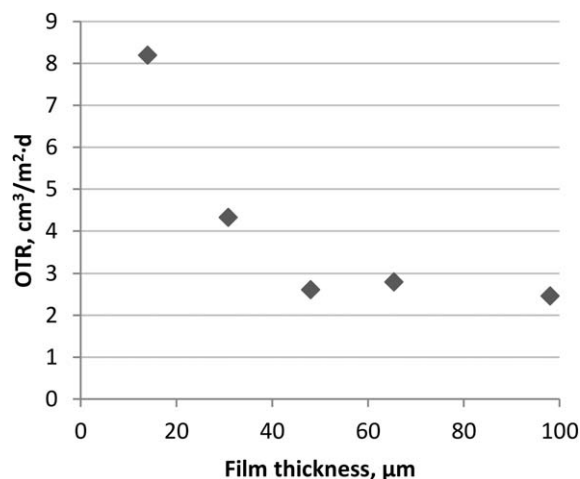


Figure 5. OTR values of EPVOH films at 80% RH as a function of film thickness. Average of two measurements.

films, assuming 0% RH inside the cups, and multiplying the value obtained with the actual film thickness. Plotting the (WVP) in $\text{g}/\text{Pa}\cdot\text{s}\cdot\text{m}$ at 80% RH against film thickness confirmed a linear relationship ($r^2 = 0.99$), which is commonly seen with hydrophilic films.³⁰ McHugh *et al.* explained this effect by the non-linear nature of hydrophilic film sorption isotherms due to increased resistance to mass transfer with increased film thickness.³⁰

Figure 4 shows the WVTR values of 100 μm thick films as a function of relative humidity for the selected polymer grades. The transmission rate trends are in line with expectations in that the LDPE and PET reference films (30 and 12 μm thickness, respectively) are unaffected by RH, whereas the steepest increase in WVTR which started at about 80% RH was found for the PVOH film. At the highest relative humidity (90% RH), a clear difference between the polymers was observed; the EPVOH grade was the most effective in suppressing the increased transmission of water vapor molecules and so was selected for analysis by other techniques with respect to filler addition.

Additional WVTR measurements at closer RH intervals (70, 75, 80, and 85%; Figure 4-insert) confirmed that the RH level at which the differences become appreciable is 80% RH. Analysis of the moisture uptake at different RHs showed that PVOH absorbs moisture more rapidly than EPVOH, especially at $\text{RH} \geq 80\%$,²⁹ thus opening a path for more rapid permeation of water vapor through the film structure.

Oxygen Transmission Rate

The OTR values were also found to level out at a film thickness around 50 μm when measured at 80% RH (Figure 5). The calculated OP values were found to follow an almost linear ($r^2 = 0.90$) increase with thickness. The similar trends observed in the WVTR and OTR data reflects the fact that they are both dependent on the amount of water present in the films (and thus polymer swelling); this is discussed further in a second paper by the authors²⁹ together with the effects of the clay fillers on oxygen and water vapor barrier properties as well as their distribution within the selected polymers.

Figure 6 shows the OTR as a function of relative humidity for the three polymer grades with film thickness of 100 μm . The results follow the same trends as in the WVTR measurements, with an increase in the oxygen transmission rate starting at around 80% RH.

Concurrent with the WVTR data, EPVOH provided the highest oxygen barrier properties at high RH compared to the other two grades. Moreover, the OTR value for EPVOH was significantly lower (by over an order of magnitude) compared with the other two polymers.

The corresponding OTR values recorded for the reference films were $1278 \text{ cm}^3 \text{ m}^{-2} \text{ d}^{-1}$ (LDPE) and $19 \text{ cm}^3 \text{ m}^{-2} \text{ d}^{-1}$ (PET) and were unaffected by RH (film thicknesses of 30 and 12 μm , respectively). Divided through by film thickness to express OTR values as oxygen permeability, the values were $378 \text{ cm}^3 \text{ cm}^{-1} \text{ m}^{-2} \text{ d}^{-1}\cdot\text{bar}$ (LDPE), $2.2 \text{ cm}^3 \text{ cm}^{-1} \text{ m}^{-2} \text{ d}^{-1}\cdot\text{bar}$ (PET), $11.3 \text{ cm}^3 \text{ cm}^{-1} \text{ m}^{-2} \text{ d}^{-1}\cdot\text{bar}$ (PVOH), and $2.4 \text{ cm}^3 \text{ cm}^{-1} \text{ m}^{-2} \text{ d}^{-1}\cdot\text{bar}$ (EPVOH). This means that the OP of EPVOH (at 80% RH) was more than two orders of magnitude lower than for LDPE, and comparable to PET.

Hydrophobic Character of Film Surfaces

The measured contact angles for the various test liquids and the corresponding total surface energies with their components for the films without fillers are shown in Table III. The total surface energies (γ_s) for the LDPE and PET reference films were 42.4 and 45.2 mJ m^{-2} , respectively. The relatively high γ_s and weak polarity ($\gamma_s^{AB} \sim 1.9 \text{ mJ m}^{-2}$) of the LDPE film compared to tabulated data (γ_s 33.0 and γ_s^{AB} 0 mJ m^{-2})²² is attributed to the oxidation of the surface by Corona discharge. The value of γ_s for the PET reference film lies close to values commonly given in the literature. PVOH and EPVOHc exhibited similar contact angles for each of the three test liquids and consequently similar γ_s values of about 49 mJ m^{-2} . EPVOH showed higher contact angles for water and ethylene glycol (i.e., the polar test liquids) than PVOH or EPVOHc, and hence a lower γ_s (47 mJ m^{-2}). van Oss²² reported values for poly(vinyl alcohol) with γ_s of 42 mJ m^{-2} , $\gamma_s^{LW} = 42$, $\gamma_s^+ = 0$ and γ_s^- in the range 17–57 mJ m^{-2} when measured at 20°C. However, a strict comparison with

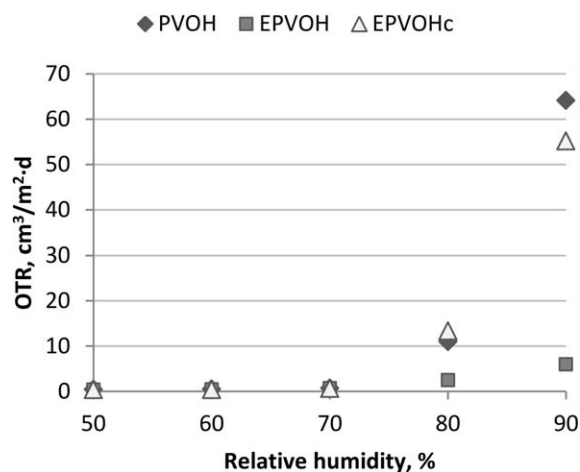


Figure 6. OTR of PVOH and EPVOH films as a function of relative humidity. Average of two measurements.

Table III. Top: Contact Angles of Polymer Films with Various Test Liquids. Average from Six Measurements with Standard Deviation. Bottom: Resulting Surface Energies for the Solid Surfaces and Their Apolar and Polar Components

Liquid	Contact angle (°)							
	Polymer films					Clay-polymer films (12 pph)		
	PVOH	EPVOH	EPVOHc	LDPE	PET	Q-MMT	C-MMT	Na-MMT
Water	58.1 ± 3.0	67.8 ± 2.3	59.3 ± 1.8	82.9 ± 3.2	65.9 ± 2.6	65.4 ± 1.0	72.7 ± 0.6	77.2 ± 2.6
Ethylene glycol	25.8 ± 0.7	34.1 ± 1.3	23.8 ± 2.3	61.8 ± 0.4	54.1 ± 1.5	33.7 ± 2.9	35.7 ± 1.7	29.6 ± 0.7
Methylene iodide	29.0 ± 1.3	31.5 ± 1.3	29.9 ± 0.6	38.2 ± 1.6	36.7 ± 2.4	38.3 ± 1.6	37.4 ± 0.7	41.8 ± 3.5
Surface energies (mJ m ⁻²)								
γ_s	49.2	47.2	49.6	42.4	45.2	45.4	45.0	43.4
γ_s^{LW}	44.6	43.6	44.3	40.5	41.2	40.5	40.9	38.0
γ_s^{AB}	4.6	3.6	5.3	1.9	3.9	4.9	4.9	4.5
γ_s^+	0.29	0.30	0.42	0.13	0.18	0.46	0.46	1.68
γ_s^-	18.5	10.8	16.6	6.7	21.6	13.3	13.3	3.0

The last three columns refer to EPVOH films with 12 pph Q-MMT, C-MMT, and Na-MMT, respectively.

tabular data requires films prepared using the same method, and measurements performed under the same conditions, with the same test liquids. EPVOH showed a lower polar (γ_s^{AB}) character than PVOH and EPVOHc but similar to that of PET. The lowest polar character was, as expected, shown for the LDPE film.

Figure 7 shows the dataset representing normalized contact angle of water, relative to that of the unfilled film, as a function of filler concentration for the three clays. The average contact angles for water from the six replicates recorded on EPVOH-clay composite films expressed standard deviations within ± 3.9 . The contact angle did not change markedly with the addition of Na-MMT and C-MMT, presumably because the top-most surface properties are dominated by the polymeric matrix; this could be anticipated because of the likelihood of the polymer to adsorb on the clay surface. A similar decrease in contact angle was observed with addition of 3–12 pph Q-MMT, showing a

more polar surface and is attributed to enrichment of excess organomodifier at the film surface.

Because the variations in contact angles with water and different clay concentrations were low within each clay series, surface energies from all three test liquids were determined using only the composite films comprising 12 pph filler (Table III).

The total surface energies (γ_s) were quite similar between the three clay composite films and slightly lower than the pure EPVOH. Q-MMT and C-MMT composites showed similar values of γ_s^{LW} , whereas a lower value was obtained for Na-MMT indicating a lower apolar character for the latter, presumably reflecting the differences in elemental composition and CEC of the clays.²⁹ The polar character (γ_s^{AB}) was lower for the unfilled film than for all three clay composite films. The tendency to act as an electron donor (γ_s^-) was lower for C-MMT and Na-MMT composite films compared to the pure EPVOH, whereas that of the Q-MMT composite film was higher than the unfilled film.

The addition of a nonpolar organomodifier as in the case of Q-MMT could be expected to result in a more non-polar surface of the composite film, but the opposite effect was observed here, i.e., a lower γ_s^{LW} and higher γ_s^{AB} for the Q-MMT composite film compared to the pure EPVOH film. This is possibly explained by the hydrophobic Q-MMT particles being located in the bulk of the film combined with the enrichment of excess surfactant modifier at the film surface, the increased polarity could arise from the polar ammonium head groups being preferentially directed towards the surface of the film, whilst the long alkyl chains reside in the film interior. The distribution of different species throughout the film is the topic for an ongoing research study.²⁹

Mechanical Properties

Figure 8 shows (a) the Young's modulus (E), (b) the tensile strength (stress at break, σ_b) and (c) the elongation at break (strain at break, ϵ_b) for EPVOH films as a function of filler content for the different clays. E increased strongly with increased filler content from about 1580 MPa for the unfilled film to

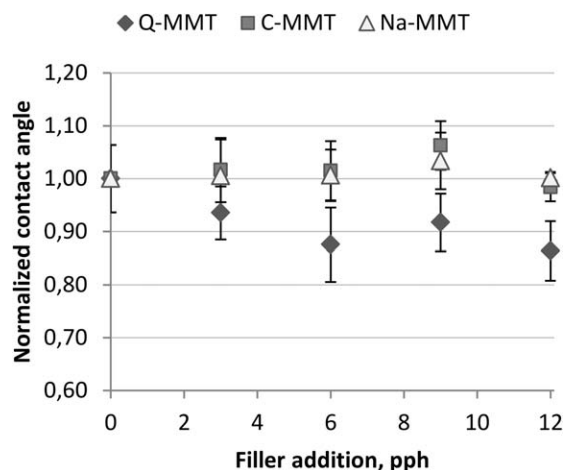


Figure 7. Normalized contact angles to water for EPVOH films as a function of filler addition. Average of six measurements with standard deviation.

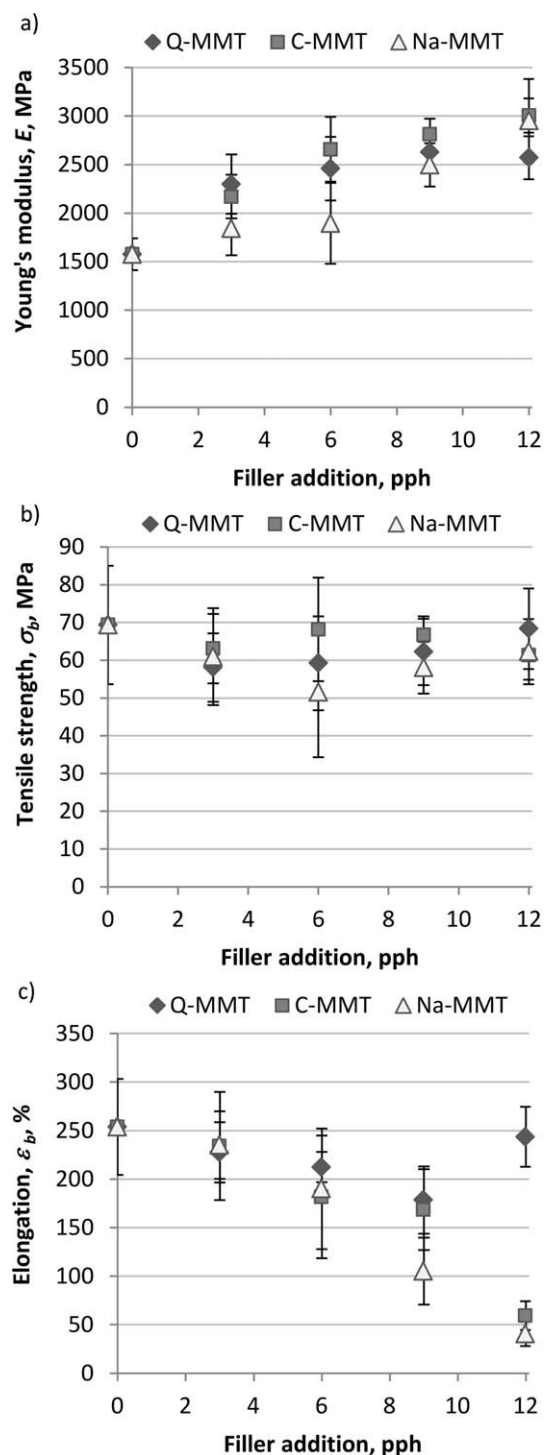


Figure 8. (a) Young's modulus, (b) tensile strength, and (c) elongation at break as a function of filler content for EPVOH films. Average from 12 measurements. Error bars represent standard deviations.

about 3000 MPa at 12 pph C-MMT or Na-MMT. For Q-MMT, the E values began to level out at around 2500 MPa with a clay loading of 6 pph or higher.

At the lowest addition level, the modulus was slightly higher for Q-MMT than for the corresponding composite comprising Na-MMT, but similar to C-MMT. Chang *et al.* reported an analo-

gous effect on the modulus when comparing organomodified montmorillonite with a Na-exchanged counterpart and explained this effect by promotion of a better orientation of the PVOH chains in a composite due to the presence of flexible alkyl groups in the organomodified montmorillonite.²⁶ The modulus of a composite material can in essence be regarded as the combined moduli of each individual component, where montmorillonite itself exerts an inherent modulus of 170 GPa (supplier information). In addition, modulus as well as tensile strength is also dependent on the polymer crystallinity, how well the two components bond together and in the case of these two factors being equal the extent of clay dispersion, i.e. intercalated or exfoliated.^{12,31} An increase in modulus with small additions of clay and exfoliation can therefore be explained by nano-scale reinforcement due to the enhanced interfacial area of montmorillonite.³¹ McGlashan and Halley also pointed out that at high clay loadings and with intercalation or microparticles, a higher amount of tactoids acting as stress focal points and potential sites for mechanical failure may emerge.³¹ The relatively high values of Young's modulus for the EPVOH/Q-MMT composite films over the entire range of filler additions is thus somewhat unexpected since XRD analysis indicated less well dispersed clay platelets in this case,²⁹ probably the formation of a microcomposite. The Q-MMT composites thus expressed a less pronounced enhancement in interfacial area compared to Na-MMT or C-MMT composites, and presumably an increased risk of failure at high clay loadings.

The tensile strength did not show any significant variations as a function of filler addition. For C-MMT the σ_b values varied between 60 and 70 MPa, with no clear trend related to the filler level. For the other two clays, a weak minimum was found at 3 pph Q-MMT and at 6 pph Na-MMT, respectively. Strawhecker and Manias¹⁶ reported that σ_{max} of PVOH composite films were rather insensitive to the filler concentration in the range 0–10 wt % MMT whereas Chang *et al.* found that the ultimate tensile strength of poly(vinyl alcohol) hybrids increased from ~105 to 175 MPa with increased clay content from 0 to 8 wt %.²⁶ However, they also showed a maximum in tensile strength with 6 wt % clay modified with 12-aminoauric acid ammonium chloride that reduced at higher clay loadings and was ascribed to agglomeration of organoclay particles. The M_w of the polymer should also have impact on the mechanical properties at different filler levels but unfortunately the M_w of the PVOHs used were not stated in any of the reports cited above.

The elongation at break was high for the unfilled EPVOH film, about 250%, which is higher than elongation values around 200% that have been reported for fully hydrolyzed PVOH grades with an intermediate degree of polymerization¹⁹ and for EVOH films with 27 mol % ethylene.⁷ With increasing addition of C-MMT and Na-MMT the ϵ_b decreased rapidly, this was more evident for Na-MMT and ϵ_b values reached below 50% at 12 pph Na-MMT. A similar reduction was reported for PVOH-MMT composite films by Strawhecker and Manias¹⁶ and by Chang *et al.*²⁶ Thus, addition of C-MMT and Na-MMT fillers strongly increases the brittleness of the films. However, the Q-MMT films showed ϵ_b values maintained above 170% at all

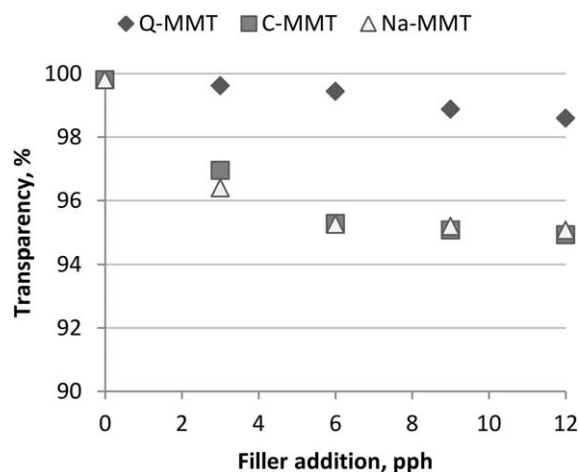


Figure 9. Transparency of composite films as a function of filler addition.

filler levels. The steep increase in ϵ_b at the highest addition of the organoclay is unexpected since a high value of ϵ_b is often associated with a low modulus or tensile strength or vice versa. However, McGlashan and Halley also reported a simultaneous increase in Young's modulus and strain at break with increased organoclay load when added to starch-polyester blends and related this to the formation of a more amorphous blend that deforms plastically rather than failing through brittle fracture.³¹ However, evidence of such a change in behavior could not be extracted directly from stress-strain curves in the present study and a detailed investigation would require microscopic analysis of the fractured surfaces in combination with a proper evaluation of film crystallinity. With 12 pph Q-MMT, ϵ_b occurred at the same level as for the unfilled EPVOH while E was maintained at about 1000 MPa higher than for pure EPVOH [Figure 8(a)]. This finding may be related to a plasticizing effect of the surfactant chains at high organoclay loadings.⁹

Transparency

The transparency of the pure EPVOH film was 99.8% whilst values for LDPE, PET and PVOH reference films were 97.7, 99.5, and 99.8%, respectively. By visual inspection, it was evident that the films became slightly hazy when clay was added and that the transparency reduced with increased filler addition. It could be noted that composite films with 3 pph C-MMT or Na-MMT were visually comparable to that of the LDPE film, with only slightly lower ability to see through the former films due to their higher thickness. This observation is also supported by their similar percentages of transparency (97.0 and 96.4% for C-MMT and Na-MMT, respectively).

The decrease in transparency with increased filler content was much more pronounced with the C-MMT and Na-MMT grades than with Q-MMT (Figure 9). The formation of opaque films is governed by the presence of particles that are larger than the wavelength of visible light, i.e. particles large enough to effectively hinder the transmission of light through the film. Strawhecker and Manias¹⁶ observed reduced transmittance of UV light with increased load of clay and assigned this to the lateral size of montmorillonite particles. An even distribution of single clay layers throughout the film and arrangement of the platelets

parallel to the surface of the film would be more effective in hindering the light from being transmitted through the film, similarly to the theories for formation of tortuous paths for permeating molecules.³² In contrast, a random distribution of single clay layers at low loadings with random orientation would lead to a more transparent film. Q-MMT showed the smallest effect on opaqueness despite having the largest layer diameter (500 nm) suggesting the presence of any single clay layers, clay-layer stacks or agglomerated clay-layer stacks were randomly distributed through the films. It should be considered that ~43 wt % of Q-MMT consists of organic material (value obtained from thermogravimetric analysis) and so there is effectively less clay present in these composites compared with addition of an equal weight fraction of C-MMT or Na-MMT. However, even if this was accounted for, the transparency values were still significantly higher than with the other clays. In addition, since the transparency was monitored over a relatively large area of the film surface (ϕ 30 mm gives an illumination area of >700 mm²) for each reading, the potential presence of regions rich in clay agglomerates, i.e. large particles that would have a major impact on the light transmitted, are confidently eliminated in the evaluation. Thus, the low impact of Q-MMT compared to Na-MMT and C-MMT on the film transparency as well as the lack of visible agglomerates indicates that the clay was evenly distributed on a sub-micron level, further investigation²⁹ has shown that the Q-MMT clay is not exfoliated, but intercalated.

Color

Visually, the films appeared increasingly yellow in color with increasing filler addition, a trend which was strongest for the films containing C-MMT filler, followed by Q-MMT and finally Na-MMT. No changes in the spectral reflectance curves in the range 540–740 nm were noted for any of the composite samples when compared to EPVOH, but differences were observed in the range 360–540 nm (Figure 10). Similar findings were reported from UV-vis transmittance spectra of PVOH/Na-MMT composites in the visible region (400–700 nm).¹⁶ The largest reflectance differences in the EPVOH composites were found in the low wavelength range, i.e. 360–440 nm, which corresponds to the upper ultraviolet region (360–380 nm) and the violet region (380–440 nm) of the visible spectrum. Within these ranges, the reflectance was found to decrease with increased content of filler, but remained constant at 9 and 12 pph for the Q-MMT and C-MMT samples indicating a saturation level was reached. Consistently, the effect on reflectance from the clays in the low wavelength range was highest for C-MMT, followed by Q-MMT and Na-MMT. Increased reflection of yellow light by the incorporation of fillers corresponds to an increased absorption of the complementary color, violet-blue light; the reflectance in this wavelength range therefore decreased with increasing amount of clay particles having a yellow tint. The absorption of light is also related to particle size, but no correlation was observed with respect to the clays diameter or perceived extent of exfoliation, intercalation or presence of micro-particles.

The color differences observed in composite films were compared to the color properties of the pure clay powders. The

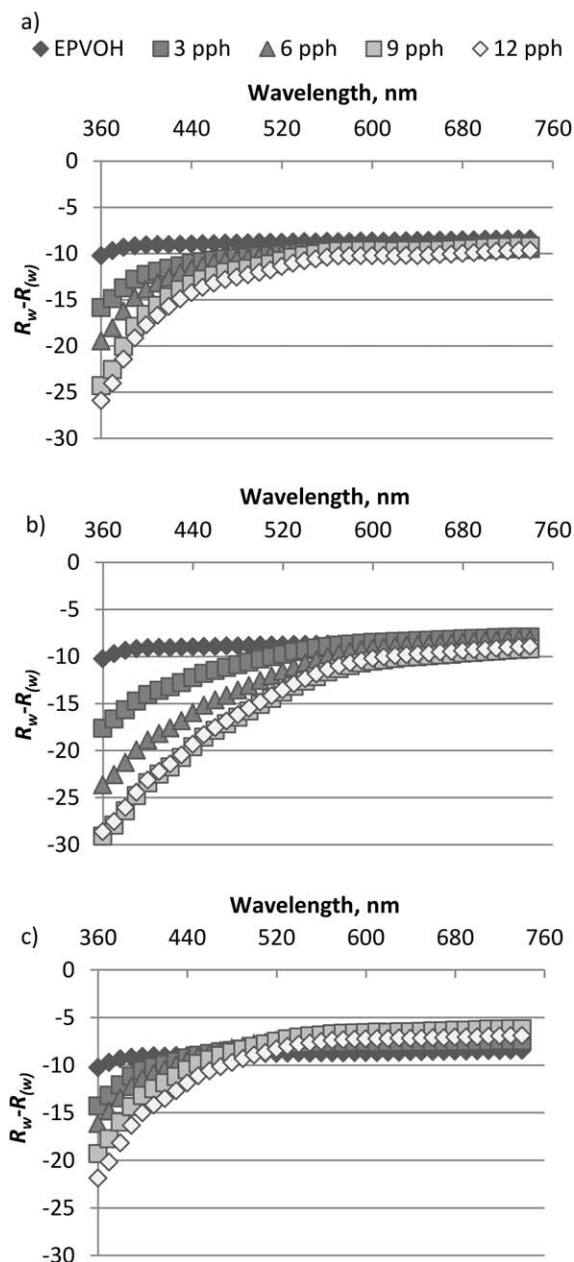


Figure 10. Reflectance curves for composite films comprising (a) Q-MMT, (b) C-MMT, and (c) Na-MMT.

shape of the reflectance curves for Na-MMT and Q-MMT were similar over the entire range of wavelengths and their lightness values, L^* , which are related to reflectance in the mid-range of the visible spectrum³³ were around 86. The C-MMT clay, however, showed lower reflectance at all wavelengths and a lower L^* value of 75. Both Q-MMT and Na-MMT showed negative a^* values with Na-MMT ($a^* -0.94$) exhibiting a more greenish shade than Q-MMT ($a^* -0.67$). C-MMT on the other hand showed redness ($a^* 1.44$). All three clays had positive b^* values; 11.44 (Q-MMT), 13.36 (C-MMT), and 10.43 (Na-MMT) supporting a measure of their yellowness. The color differences are related to the presence of iron and/or other colored ion impurities in the lattice structure of clay (or mineral impurities)

rather than on cation exchange sites. Corresponding color differences were also reflected in the visual appearance of the films comprising different fillers.

Gloss

Measurements of gloss determined from the film side in contact with air are presented in Figure 11 for the EPVOH composite films containing 3 pph filler alongside those of the pure polymer films. EVOH films are recognized for their very high gloss.⁷ Indeed the EPVOH films exhibited 104 gloss units on average, almost equal to the highly glossy PET reference film and slightly higher than the PVOH film. LDPE on the other hand had low gloss (around 20). EPVOH composite films containing the hydrophobic modified Q-MMT showed high gloss over the entire range of loadings (23–86 gloss units for 12–3 pph Q-MMT, respectively) whereas the respective films containing C-MMT had a semi-glossy appearance (7–12 gloss units) and the Na-MMT films had a matte finish (3–4 gloss units).

Gloss is a property that is controlled by the topmost surface properties. Incorporation of fillers may lead to a slight increase in the micro scale surface roughness which could partially explain the observed decrease in gloss compared to the unfilled film. The data may also give some information about the distribution of clay particles. The lower gloss obtained for composite films comprising C-MMT and Na-MMT indicate the location of clay particles near the topmost surface whereas that for the Q-MMT composite indicates the clay particles are below the topmost surface, which was evidenced also by FTIR analysis²⁹ of the films. This correlates with the contact angle measurements in that the Q-MMT had more polar character and was more similar to that of the pristine EPVOH.

Summary

The hydrophilic C-MMT and Na-MMT clays were readily dispersed in an aqueous solution of EPVOH. Na-MMT was observed to have a higher impact on the dispersion viscosity, indicative of a stronger interaction with EPVOH as compared to C-MMT. Q-MMT however seemed to be less compatible with this hydrophobically modified polymer. Analysis of water

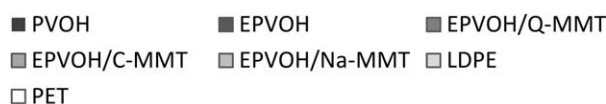


Figure 11. Gloss values for reference films and EPVOH composite films comprising 3 pph filler.

vapor- and oxygen transmission rates demonstrated that the moisture sensitivity of the polymers became apparent at 80% RH but that EPVOH provided lower transmission rates compared to the conventional PVOH and EPVOHc grades. Both WVTR and OTR of EPVOH films started to level out at a film thickness equal to and greater than 50 μm . EPVOH films provided an oxygen barrier comparable to that of a commercial PET packaging film. Investigation of the film surfaces by contact angle measurements revealed a lower polar character of EPVOH compared to that of PVOH. Addition of C-MMT or Na-MMT in the range 3–12 pph did not change the contact angle to water for EPVOH to any greater extent, hence suggesting that the topmost film surface is dominated by the polymeric matrix. The finding that a film with 12 pph Q-MMT showed higher polarity compared to the unfilled EPVOH film was ascribed to enrichment of excess surfactant modifier at the film surface.

Addition of 12 pph C-MMT or Na-MMT resulted in an almost twofold increase in Young's modulus of the EPVOH film. However, the elongation at break decreased rapidly from about 250% for the unfilled film to about 50% at the highest load of these clays. On the other hand, addition of Q-MMT resulted in ε_b values above 170% at all filler levels, while E was maintained around 2500 MPa. This simultaneous impact on ε_b and E might be related to plasticization caused by the excess surfactant present in Q-MMT.

Incorporation of the bentonites caused a stronger reduction in transparency in the case of C-MMT and Na-MMT thus indicating a more even distribution of clay mineral platelets within these composites. In contrast, the high transparency of Q-MMT films at all addition levels suggests a random distribution of clay mineral stacks with a high level of light transmission through regions poor in filler material. The reflectance of composite films in the low wavelength range was found to decrease with increased filler addition and the effect was strongest for the C-MMT clay which exhibited the most intense color in terms of redness and yellowness.

The semi-glossy and matte surfaces of C-MMT and Na-MMT composite films respectively indicated the location of clay particles near the topmost surface in these cases whereas the high gloss for Q-MMT composite films suggested that the clay particles were more deeply buried within the films.

CONCLUSIONS

This study showed that a hydrophobically modified poly(vinyl alcohol) (EPVOH) was more effective than conventional PVOH in terms of water vapor and oxygen barrier properties at high relative humidities. EPVOH films having oxygen permeability comparable to that of a biaxially oriented PET packaging film even at 80% RH could be produced. Composite films with three different montmorillonites were successfully formed, all of which showed a strong increase in Young's modulus with increased addition of clay. The organomodified clay proved to be effective at low addition levels in terms of maintaining high elongation at break, high transparency (>98%) and high gloss. Addition of high loads of Q-MMT are believed to form aggregates or microcomposites, in which the layered silicate is present

as tactoids distributed in the polymer matrix but without separation of the individual layers.

The study also demonstrated how relatively simple and rapid measurement techniques like spectrophotometry and surface gloss can give useful information about the effects of various montmorillonite types and clay loadings on the color, transparency and distribution of filler material when incorporated in a polymer film.

ACKNOWLEDGMENTS

The authors acknowledge Professor Chris Breen for valuable comments on this manuscript.

REFERENCES

1. Hodge, R. M.; Bastow, T. J.; Edward, G. H.; Simon, G. P.; Hill, A. *J. Macromolecules* **1996**, *29*, 8137.
2. Breen, A. F.; Breen, C.; Clegg, F.; Döppers, L.-M.; Khairuddin, L. M.; Sammon, C.; Yarwood, J. *Polymer* **2012**, *53*, 4420.
3. Ashley, R. H. In *Polymer Permeability*; Comyn, J., Ed.; Elsevier Applied Science Publishers: Essex, UK, **1985**; p 269.
4. Krochta, J. M.; deMulder-Johnston, C. *Food Technol.* **1997**, *51*, 61.
5. Johansson, C.; Bras, J.; Mondragon, I.; Nechita, P.; Plackett, D.; Šimon, P.; Gregor Svetec, D.; Virtanen, S.; Giacinti Baschetti, M.; Breen, C.; Clegg, F.; Aucejo, S. *BioResources* **2012**, *7*, 2506.
6. Leonard, M. W. In *Yam, K. L., The Wiley Encyclopedia of Packaging Technology*, 3rd ed.; Wiley: Hoboken, NJ, **2009**; p 98.
7. Foster, R. H. In *The Wiley Encyclopedia of Packaging Technology*, 3rd ed.; Yam, K. L., Ed.; Wiley: Hoboken, NJ, **2009**; p 418.
8. Weilbacher, R. In *PTS Workshop Innovative Packaging*, GV 773, PTS; Kleebauer, M., Sangl, R., Ed.; Munich: PTS, **2007**; p 6.
9. LeBaron, P. C.; Wang, Z.; Pinnavaia, T. *J. Appl. Clay Sci.* **1999**, *15*, 11.
10. Mittal, V. In *Nanocomposites with Biodegradable Polymers: Synthesis, Properties, and Future Perspectives*; Mittal, V., Ed.; Oxford University Press: Oxford, UK, **2011**; p 1.
11. Park, H.-M.; Li, X.; Jin, C.-Z.; Park, C.-Y.; Cho, W.-J.; Ha, C.-H. *Macromol. Mater. Eng.* **2002**, *287*, 553.
12. Alexandre, M.; Dubois, P. *Mater. Sci. Eng.* **2000**, *28*, 1.
13. Sinha, R. S.; Bousmina, M. *Prog. Mater. Sci.* **2005**, *50*, 962.
14. Paul, M.-A.; Alexandre, M.; Degée, P.; Henrist, C.; Rulmont, A.; Dubois, P. *Polymer* **2003**, *44*, 443.
15. Carrado, K. A.; Thyagarajan, P.; Elder, D. W. *Clays Clay Miner.* **1996**, *44*, 506.
16. Strawhecker, K. E.; Manias, E. *Chem. Mater.* **2000**, *12*, 2943.
17. Chen, B.; Evans, J. R. G. *Carbohydr. Polym.* **2005**, *61*, 455.
18. Xie, F.; Halley, P. J.; Avérous, L. In *Nanocomposites with Biodegradable Polymers: Synthesis, Properties and Future*

- Perspectives; Mittal, V., Ed.; Oxford University Press: Oxford, UK, **2011**; p 234.
19. Toyoshima, K. In Polyvinyl Alcohol Properties and Applications; Finch, C. A., Ed.; Wiley: New York, **1973**; p 339.
20. Johansson, C. In Nanocomposites with Biodegradable Polymers: Synthesis, Properties and Future Perspectives; Mittal, V., Ed.; Oxford University Press: Oxford, UK, **2011**; p 348.
21. Robertson, G. L. Food Packaging Principles and Practice, 2nd ed.; Taylor & Francis Group: Boca Raton, FL, **2006**.
22. van Oss, C. J. Interfacial Forces in Aqueous Media; Marcel Dekker: New York, **1994**.
23. Bastow, T. J.; Hodge, R. M.; Hill, A. J. *J. Membr. Sci.* **1997**, *131*, 207.
24. de Souza, C.; Tavares, M. I. B. *J. Appl. Polym. Sci.* **1998**, *70*, 2457.
25. McMurry, J. Organic Chemistry; Brooks/Cole Publishing Company: Belmont, CA, USA, **1992**.
26. Chang, J.-H.; Jang, T.-G.; Jin Ihn, K.; Lee, W.-K.; Soo Sur, G. *J. Appl. Polym. Sci.* **2003**, *90*, 3208.
27. Sinha, R. S.; Okamoto, K.; Okamoto, M. *Macromolecules* **2003**, *36*, 2355.
28. Toyoshima, K. In Polyvinyl Alcohol Properties and Applications; Finch, C. A., Ed.; Wiley: New York, **1973**; p 17.
29. Johansson, C.; Clegg, F. *J. Appl. Polym. Sci.* Submitted.
30. McHugh, T. H.; Avena-Bustillos, R.; Krochta, J. M. *J. Food Sci.* **1993**, *58*, 899.
31. McGlashan, S. A.; Halley, P. J. *Polym. Int.* **2003**, *52*, 1767.
32. Bharadwaj, R. K. *Macromolecules* **2001**, *34*, 9189.
33. Hubbe, M. A.; Pawlak, J. J.; Koukoulas, A. A. *BioResources* **2008**, *3*, 627.